PTEP

Prog. Theor. Exp. Phys. **2014**, 103D01 (14 pages)
DOI: 10.1093/ptep/ptu131

Pion-induced reactions for charmed baryons

Sang-Ho Kim[1], Atsushi Hosaka[1,2,*], Hyun-Chul Kim[3], Hiroyuki Noumi[1], and Kotaro Shirotori[1]

[1]*Research Center for Nuclear Physics (RCNP), Osaka University, Ibaraki, Osaka 567-0047, Japan*
[2]*J-PARC Branch, KEK Theory Center, Institute of Particle and Nuclear Studies, KEK, Tokai, Ibaraki 319-1106, Japan*
[3]*Department of Physics, Inha University, Incheon 402-751, Republic of Korea*
*E-mail: hosaka@rcnp.osaka-u.ac.jp

Received May 20, 2014; Revised August 12, 2014; Accepted August 26, 2014; Published October 6, 2014

We study pion-induced binary reactions for charmed baryons, $\pi + N \to D^* + B$, where B is a charmed baryon of ground or excited state. First we estimate charm production rates in comparison with strangeness production using a Regge model, which is dominated by vector (D^* or K^*) Reggeon exchange. Then we examine the production rates of various charmed baryons B in a quark–diquark model. We find that the production of excited states is not necessarily suppressed, a sharp contrast to strangeness production, which is a unique feature of the charm production with a large momentum transfer.

Subject Index D32

1. Introduction

Observations of new hadrons have been stimulating diverse activities in hadron physics; see, for instance, Ref. [1]. Evidence first observed at electron facilities such as KEK, SLAC, and BES [2–7] is now receiving strong support from recent LHCb experiments [8,9]. Many new hadrons have been found near the threshold regions of charm or bottom quarks. Intuitively, excited heavy quarks break a string followed by creation of a light quark–antiquark pair, forming exotic hadrons with multiquarks near the threshold. To understand the features of the new findings, therefore, requires systematic studies of the dynamics from light to heavy quark regions.

So far, many of the new observations have been made for mesons. In contrast, not much progress has been achieved for baryons. In fact, the number of known heavy quark baryons is much less than that of light quark baryons. The study of charmed baryons is important not only for heavy but also for light quark dynamics, which in turn will be linked to the physics of the new hadrons and eventually to the unsolved problems of quantum chromodynamics (QCD).

From the above background, an experimental proposal is being made for the new pion beam facility at J-PARC [10]. The expected pion energy will reach over 20 GeV in the laboratory frame, which is sufficient to excite charmed baryons up to around 1 GeV. This is a challenging experiment since there has been no experiment since the one at Brookhaven almost thirty years ago [11,14]. The relevant reaction has been chosen, i.e.,

$$\pi + N \to D^* + B, \tag{1}$$

where D^* is the charmed vector meson and B a charmed baryon. Here B is a low-lying baryon of either ground or excited state. The reason that D^* is selected in the reaction is due to an experimental advantage as compared to the production of the D meson.

The purpose of this paper is to perform a theoretical study for the above reaction, while experimental feasibility is now under investigation. The study of such reactions is a challenging problem, because 1) not many studies have been performed so far, 2) production rates should reflect the structure of charmed baryons, and, furthermore, 3) the charm production mechanism from the threshold region to the region of a few GeV is not well understood.

The structure of charmed baryons has been studied in a quark model [12,13]. One of the unique features due to the presence of a charm quark is the so-called isotope shift. In the light flavor sector where the three quarks have a similar mass, the two independent internal motions of the ρ and λ modes are degenerate, which in the presence of a heavy quark split and appear differently in the spectrum. This already seems to be the case in the strange baryons, as seen in the inversion of the mass ordering in $\Sigma(1775)$–$\Lambda(1830)$. It is then very important to perform systematic studies from the light to the heavy flavor sectors.

This paper is organized as follows. In Sect. 2, we estimate the rate of charm production using a Regge model in comparison with strangeness production. In Sect. 3, we compute the production rates of various charmed baryons B, up to the orbital excitations of a d-wave ($l = 2$) in a heavy quark–diquark description of B. The result indicates that the production of excited states B is not necessarily suppressed in comparison with strange hyperon production. In Sect. 4, we discuss prospects and summarize the present work.

2. Estimation of cross sections

Let us consider forward angle scattering for the reaction (1), where the t-channel dynamics as shown in Fig. 1 (left panel) dominates, and the Regge model is expected to be a good prescription. Many experiments have shown that the cross sections are of forward peak (diffractive) at energies beyond a few GeV, which is also the region of charm production. For strangeness production, a reaction relevant to the present study, $\pi + p \to K^* + B_s$, was performed long ago [15]. This has clearly shown a forward peak structure, which indicates the t-channel mechanism in the forward angle region.

In the Regge theory [16], the scattering amplitude is first expanded into partial waves in the t-channel scattering region ($s < 0, t > 0$), which is then analytically continued to the physical region of s-channel scattering ($s > 0, t < 0$). The sum over integer angular momentum l is then equivalently expressed by the Regge pole terms, which are the residues of the scattering amplitude in the complex angular momentum plane. The pole is a function of t and is identified with a Regge trajectory $\alpha(t)$. The amplitude expressed by the Regge poles is then referred to as the Reggeon exchange amplitude.

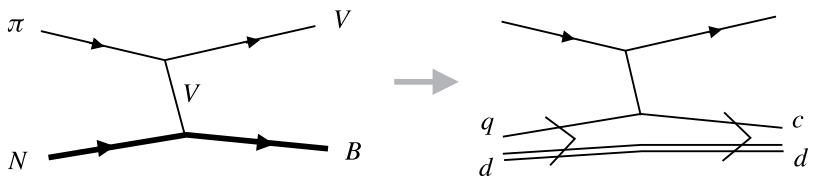

Fig. 1. Left: A t-channel process (vector Reggeon exchange) for the $\pi + N \to V + B$ reaction, where $V = D^*, K^*$. Right: Quark–diquark structure is shown for the nucleon and charmed baryons, which is discussed in Sect. 3.

The advantage of the Regge theory is that it determines the asymptotic behavior of the cross section of binary reactions,

$$\frac{d\sigma}{dt} \to s^{2\alpha(t)-2}, \tag{2}$$

which describes well the observed s-dependence. The s-dependence is determined solely by the kind of Reggeon through the trajectory $\alpha(t)$, and is universal for any binary states as long as the same Reggeon is exchanged. Among various contributions of different trajectories (Reggeons), the dominant one is given by that of the largest $\alpha(t)$. For example, the vector Reggeon is more dominant than the pseudoscalar Reggeon.

For our present estimation, we employ Kaidalov's prescription for the vector Reggeon exchange [17,18],

$$\frac{d\sigma}{dt} = \frac{\text{factor}}{64\pi |\boldsymbol{p}|^2 s}\Gamma^2(1-\alpha_V(t))\left(\frac{s}{\bar{s}}\right)^2\left(\frac{s}{s_0}\right)^{2\alpha_V(t)-2}. \tag{3}$$

Here $\boldsymbol{p}$ is the relative momentum of the initial state in the center-of-mass system and $\bar{s}$ a universal scale parameter. In the present study of ratios the parameter $\bar{s}$ is not important. The other scale parameter s_0 depends on the flavors of the Reggeon, and is determined by the probabilistic picture [17],

$$s_0(\text{charm}) = 4.75\,\text{GeV}^2, \quad s_0(\text{strange}) = 1.66\,\text{GeV}^2. \tag{4}$$

For the trajectories $\alpha_V(t)$, we employ a non-linear parametrization

$$\alpha(t) = \alpha_0 + \gamma(\sqrt{T} - \sqrt{T-t}), \tag{5}$$

to realize a better fit to trajectories than the linear parametrization, where the parameters α_0, γ, and T are given for each trajectory as tabulated in Ref. [19].

In this paper, we use Eq. (3) to estimate the relative production rate of strange and charmed baryons by assuming the same strength of the overall "factor" in Eq. (3). Such an assumption should be good for heavy quark sectors, while it is not necessarily applicable in the strangeness sector. Nevertheless, we expect that it will provide useful information for the unknown quantities. One could also obtain the total cross section, but here we will not do it, because there is ambiguity in the form factor (t-dependence). In Eq. (3) we employ the one derived from Regge's method, which is analytically continued from the t-channel scattering region to the s-channel scattering region. This does not necessarily reproduce the observed t-dependence well. In fact, an alternative parametrization is possible when data are available [18,20,21]. Thus our strategy here is to investigate the forward cross section $d\sigma/dt(\theta = 0)$ for charm and strangeness production, expecting that the Regge model works best in the forward angle region.

In Fig. 2, we show $d\sigma/dt$ in arbitrary units [au] as a function of s/s_{th}, where s_{th} is the s-value at the threshold; $s_{\text{th}}(\text{strange}) = (m_B + m_{K^*})^2$ and $s_{\text{th}}(\text{charm}) = (m_B + m_{D^*})^2$. By making a plot as a function of the ratio s/s_{th}, we can directly compare the ratios of strange and charm production. Two curves are plotted in arbitrary units while keeping their ratio determined by Eq. (3). The ratio of charm to strangeness production varies from 10^{-3} near the threshold $s/s_{\text{th}} \sim 1$ to 10^{-5} at large energies $s/s_{\text{th}} \sim 10$. The expected experiments at J-PARC will be done most efficiently at $s/s_{\text{th}} \sim 2$, where the rate of charm production is smaller than strangeness production by a factor of about 10^{-4}. Therefore, if one uses the total cross section for K^* production with the ground state Λ or Σ of the

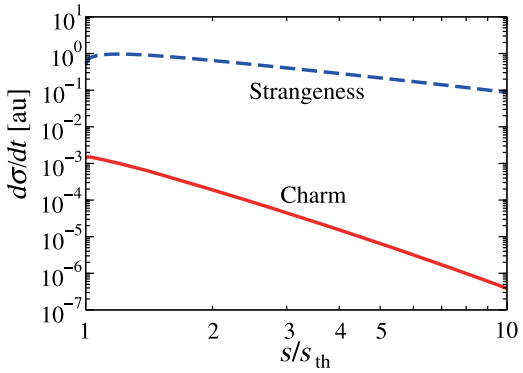

Fig. 2. Forward differential cross sections $d\sigma/dt(\theta = 0)$ as a function of $s/s_{\rm th}$, where $s_{\rm th}$ is the s-value at the threshold. Solid and dashed lines are for charm and strangeness production, respectively. Absolute values are shown in arbitrary units, but their ratio is properly computed by Eq. (3).

order of several 10 [μb] at $s/s_{\rm th} \sim 2$,[1] the expected one for charm production with Λ_c or Σ_c is of the order of several nanobahn.

So far, we have estimated the total cross section indirectly by using the ratios for $d\sigma/dt$, because, as anticipated, there are more points to be studied for the theoretical evaluation of the total cross section. We are currently working on the details, which will be discussed elsewhere.

3. Production of various charmed baryons

3.1. Quark–diquark baryons

In this section, baryons are described as two-body systems of a quark and a diquark. Charmed baryons are then composed of a heavy quark and a light diquark. The relative motion of the quark and diquark is described by the λ coordinate, one of the Jacobi coordinates of a three-body system, as shown in Fig. 3. The internal motion of the diquark as described by the other variable ρ is implicit in the quark–diquark model. Due to spin–spin interaction, the pair of ${}^3S_0^\rho$ quarks (d^0) is considered to have a lower mass than the pair of ${}^3S_1^\rho$ quarks (d^1) . In general, we can also consider internal excitations of diquarks. Furthermore, the λ and ρ modes can couple and mix. In this paper, however, we consider only λ motions of (orbitally) ground-state diquarks of the above two kinds, d^0 and d^1, because the reaction mechanism that we consider as shown in Fig. 1 (right) dominantly excites a λ mode. The quark–diquark wave functions of the λ modes are summarized in Appendix B. We have then made a tentative assignment of these states to the nominal ones listed in PDG when available [22], as shown in Table 1. We have also made arbitrary assignments of the unknown states to fill the corresponding ones by simply guessing their masses. The latter are shown in Table 1 with a * symbol.

As shown in Fig. 1, in the t-channel process, a charmed Reggeon is exchanged and couples with a quark in the initial nucleon transformed into a charm quark forming a charmed baryon in the final state. Our calculation here is performed under several assumptions.

- As in the previous section, we consider vector ($V = D^*$ or K^*) Reggeon exchanges because at high energies the V Reggeon dominates.

[1] The experimental total cross sections are 23.1 ± 4.3, 8.8 ± 2.1, 63.1 ± 7.7 [μb] for $\pi^- p$ to $\Sigma^0 K^{*0}$, $\Sigma^- K^{*+}$, ΛK^{*0}, respectively at $s/s_{\rm th} \sim 2$ [14].

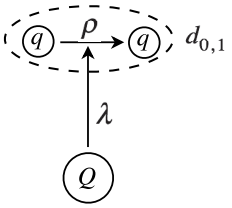

Fig. 3. λ and ρ coordinates of a three-quark system, qqQ. The light quarks qq may form a diquark d_S of spin $S = 0, 1$.

Table 1. Baryon masses M [MeV] (see text for assignment), spin-dependent coefficients C, and the ratios of production rates $\mathcal{R}$ given in Eq. (19). The second and third rows are the ratios $\mathcal{R}$ for the strange and charmed baryons, respectively, which are normalized to the ground-state Λ. They are computed at $k_\pi^{\rm Lab} = 4.2\,{\rm GeV}$ for the strange, and at $k_\pi^{\rm Lab} = 20\,{\rm GeV}$ for the charmed baryons.

$l = 0$	$\Lambda\left(\frac{1}{2}^+\right)$	$\Sigma\left(\frac{1}{2}^+\right)$	$\Sigma\left(\frac{3}{2}^+\right)$				
M [MeV]	1116	1192	1385				
	2286	2455	2520				
C	1	1/9	8/9				
$\mathcal{R}(B_s)$	1	0.04	0.210				
$\mathcal{R}(B_c)$	1	0.03	0.17				
$l = 1$	$\Lambda\left(\frac{1}{2}^-\right)$	$\Lambda\left(\frac{3}{2}^-\right)$	$\Sigma\left(\frac{1}{2}^-\right)$	$\Sigma\left(\frac{3}{2}^-\right)$	$\Sigma'\left(\frac{1}{2}^-\right)$	$\Sigma'\left(\frac{3}{2}^-\right)$	$\Sigma'\left(\frac{5}{2}^-\right)$
M [MeV]	1405	1520	1670	1690	1750	1750	1775
	2595	2625	2750	2800	2750	2820	2820
C	1/3	2/3	1/27	2/27	2/27	56/135	2/5
$\mathcal{R}(B_s)$	0.07	0.11	0.002	0.003	0.003	0.01	0.01
$\mathcal{R}(B_c)$	0.93	1.75	0.02	0.04	0.05	0.21	0.21
$l = 2$	$\Lambda\left(\frac{3}{2}^+\right)$	$\Lambda\left(\frac{5}{2}^+\right)$	$\Sigma\left(\frac{3}{2}^+\right)$	$\Sigma\left(\frac{5}{2}^+\right)$	$\Sigma'\left(\frac{1}{2}^+\right)$	$\Sigma'\left(\frac{3}{2}^+\right)$	$\Sigma'\left(\frac{5}{2}^+\right)$	$\Sigma'\left(\frac{7}{2}^+\right)$
M [MeV]	1890	1820	1840	1915	1880	2000*	2000*	2000*
	2940	2880	1840	3000*	3000*	3000*	3000*	3000*
C	2/5	3/5	2/45	3/45	2/45	8/45	38/105	32/105
$\mathcal{R}(B_s)$	0.02	0.04	0.003	0.001	0.001	0.001	0.001	0.001
$\mathcal{R}(B_c)$	0.49	0.86	0.01	0.02	0.01	0.05	0.11	0.09

- The cross section shows a forward peak. Therefore, we compute the differential cross sections only at the forward angle.
- We focus on ratios of excited charmed baryon production as compared to ground-state production.

The main issue in this section is the computation of various baryon matrix elements and their ratios. For this purpose, we follow the standard prescription of the Reggeon calculation [21]. (1) Write the Feynman amplitude assuming that the Reggeon vertices are given by that of the lowest one (band head). For vector Reggeon exchange, those of vector mesons, D^* or K^*, are employed. (2) The ordinary Feynman propagator is then replaced by the Reggeon propagator, which gives the correct

s-dependence of the cross section. Thus we introduce the following two interaction Lagrangians,

$$\mathcal{L}_{\pi VV} = f\epsilon_{\mu\nu\alpha\beta}\,\partial^\mu\pi\partial^\nu V^\alpha V^\beta, \tag{6}$$

$$\mathcal{L}_{Vqc} = g\bar{c}\gamma^\mu q V_\mu. \tag{7}$$

Here, f and g are coupling constants, and q and c denote the spinors of the light ($q = u, d$) and charm quarks, respectively. The quark vertex (7) is reflected in different baryon structures in the final state.

3.2. Amplitudes

Let us first look at the matrix element of the πVV coupling of Eq. (6),

$$\langle V(k_V)|\mathcal{L}_{\pi VV}|\pi(k_\pi)V(q)\rangle \sim 2f\epsilon_{\mu 0\alpha\beta}k_\pi^\mu k_V^0 e^\alpha e^\beta \to 2fk_V^0\vec{k}_\pi\times\vec{e}\cdot\vec{e}, \tag{8}$$

where k_π, k_V, and q are the momentum of the initial pion, of the final V, and of the exchanged V meson, respectively. $e^{\alpha,\beta}$ are the polarization vectors of either the final or the intermediate vector mesons. In these manipulations, we selected the dominant term assuming that the reaction energy is not relativistically too large as in the case for $s/s_{\rm th} \lesssim 2$, where the relative momentum in the center-of-mass frame in the final state does not greatly exceed their masses.

Next, we compute the baryon matrix element of $\mathcal{L}_{Vqc}$,

$$\begin{aligned}\langle\mathcal{L}_{Vqc}\rangle &= \langle g\bar{c}\gamma^\mu V_\mu q\rangle \\ &= g\varphi_f^\dagger\left(1, -\frac{\vec{\sigma}\cdot\vec{p}_f}{m_c+E_c}\right)\begin{pmatrix}V^0 & -\vec{\sigma}\cdot\vec{V}\\ \vec{\sigma}\cdot\vec{V} & -V^0\end{pmatrix}\begin{pmatrix}1\\ \dfrac{\vec{\sigma}\cdot\vec{p}_i}{m_q+E_q}\end{pmatrix}\varphi_i,\end{aligned} \tag{9}$$

where $\varphi_{i,f}$ are the two-component spinors for the initial light quark and the final charm quark, respectively. To proceed, we pick up only terms that contain the spatial component of the V meson, because when this V meson is contracted with another from the πVV vertex, only the spatial component survives as Eq. (8) implies. Hence we find

$$\mathcal{L}_{Vqc} \sim -g\varphi_f^\dagger\left[\left(\frac{\vec{p}_f}{m_c+E_c}+\frac{\vec{p}_i}{m_q+E_q}\right)\cdot\vec{V} + i\vec{\sigma}\times\left(\frac{\vec{p}_f}{m_c+E_c}-\frac{\vec{p}_i}{m_q+E_q}\right)\cdot\vec{V}\right]\varphi_i. \tag{10}$$

Now combining the matrix elements Eqs. (8) and (10), we can write down the scattering amplitude as

$$t_{fi} \sim 2fgk_V^0\vec{k}_\pi\times\vec{e}\cdot\vec{J}_{fi}G_V(t), \tag{11}$$

where

$$G_V(t) = \Gamma(1-\alpha(t)_V)\left(\frac{s}{s_0}\right)^{\alpha(t)_V-1} \tag{12}$$

is the Reggeon propagator, and $\vec{J}_{fi}$ the baryon transition current,

$$\vec{J}_{fi} = \int d^3x\,\varphi_f^\dagger\left[\frac{\vec{p}_f}{m_c+E_c}+\frac{\vec{p}_i}{m_q+E_q}+i\vec{\sigma}\times\left(\frac{\vec{p}_f}{m_c+E_c}-\frac{\vec{p}_i}{m_q+E_q}\right)\right]\varphi_i\,e^{i\vec{q}_{\rm eff}\cdot\vec{x}}. \tag{13}$$

Here we have defined the effective momentum transfer

$$\vec{q}_{\rm eff} = \frac{m_d}{m_d+m_q}\vec{P}_N - \frac{m_d}{m_d+m_c}\vec{P}_B, \tag{14}$$

which takes into account the recoil of the center-of-mass motion due to the change in the masses of q and c quarks [23].

To further simplify the computation, the quark momenta $\vec{p}_i$ and $\vec{p}_f$ are approximated to take a fraction of the baryon momentum,

$$\vec{p}_i \sim \frac{1}{3}\vec{P}_N,$$
$$\vec{p}_f \sim \frac{m_c}{m_c+m_d}\vec{P}_B. \tag{15}$$

Note that for the initial state the pion momentum (and hence the nucleon momentum) is sufficiently large such that the mass of the light quarks in the nucleon is neglected. Now for forward scattering where all momenta are collinear along the z-axis, only the spin current term survives in the scattering amplitude:

$$\begin{aligned} t_{fi} &\sim \left(\frac{P_B}{2(m_c+m_d)}-1\right) k_V^0 \vec{k}_\pi \times \vec{e}\cdot\left\langle f\left|\vec{\sigma}\times\hat{z}\, e^{i\vec{q}_{\rm eff}\cdot\vec{x}}\right|i\right\rangle G_V(t) \\ &= \left(\frac{P_B}{2(m_c+m_d)}-1\right) k_V^0 \left\langle f\left|\left((\vec{k}_\pi\cdot\vec{\sigma})(\vec{e}\cdot\hat{z})-(\vec{k}_\pi\cdot\hat{z})(\vec{e}\cdot\vec{\sigma})\right) e^{i\vec{q}_{\rm eff}\cdot\vec{x}}\right|i\right\rangle G_V(t), \end{aligned} \tag{16}$$

where the constant factors, which are irrelevant when taking the ratios of the production rates, are ignored. The polarization of V can be either longitudinal (z) or transverse (x, y), but the longitudinal contribution vanishes. Moreover, for the transverse polarization, the first term vanishes. Finally, we obtain a rather concise formula for the amplitude:

$$t_{fi} \sim \left(\frac{P_B}{2(m_c+m_d)}-1\right) k_V^0 k_\pi \langle f|\, \vec{e}_\perp\cdot\vec{\sigma}\, e^{i\vec{q}_{\rm eff}\cdot\vec{x}}\,|i\rangle\, G_V(t). \tag{17}$$

Here $\vec{e}_\perp$ denotes the transverse vector, and hence the transverse spin induces the transition, as expected for the vector ($J^P = 1^-$) exchange process.

3.3. Production rates

We have computed the transition amplitudes t_{fi} from the nucleon $i \sim N$ to various charmed baryons $f \sim B$. For charmed baryons, we consider all possible states including the ground, p-wave, and d-wave excitations. The production rates are computed by

$$\mathcal{R} \sim \frac{1}{\rm Flux}\times\sum_{fi}|t_{fi}|^2 \times \text{Phase space}. \tag{18}$$

Using the results of the amplitudes as shown in Appendix A, we find

$$\mathcal{R}(B(J^P)) = \frac{1}{4|\boldsymbol{p}|\sqrt{s}}\gamma^2\, K^2\, C\, |I_L|^2 \frac{q}{4\pi\sqrt{s}}. \tag{19}$$

In these expressions, C is the geometric factor of the matrix element $\langle f|\,\vec{e}_\perp\cdot\vec{\sigma}\, e^{i\vec{q}_{\rm eff}\cdot\vec{x}}\,|i\rangle$ determined by the spin, angular momentum, and total spin of the baryon, while $I_L (L = 0, 1, 2)$ contains dynamical information on the baryon wave function. K is the kinematic factor

$$K = k_V^0 k_\pi \left(\frac{P_B}{2(m_c+m_d)}-1\right) G_V(t) \tag{20}$$

and γ the following isospin overlap factor:

$$\gamma = \frac{1}{\sqrt{2}} \quad \text{for } \Lambda \text{ baryons},$$
$$= \frac{1}{\sqrt{6}} \quad \text{for } \Sigma \text{ baryons}. \tag{21}$$

By using the baryon wave functions as summarized in Appendices B and C, the geometric factors C and the production rates $\mathcal{R}$ are computed. In Table 1, results are shown for both charm and strangeness

production at the pion momentum in the laboratory frame, $k_\pi^{\rm Lab} = 20\,{\rm GeV}$ for charm production and $k_\pi^{\rm Lab} = 4.2\,{\rm GeV}$ for strangeness production. These momenta correspond to $s/s_{\rm th} = 2$ for both cases. The wave functions of strange baryons are obtained by replacing the charm quark by a strange quark. The rates $\mathcal{R}$ presented in the table are normalized by that of the lowest Λ baryon.

Herein below we make several observations.

- In general the production rates for Λ baryons are larger than for Σ baryons. This is a consequence of the SU(6) symmetry of quark–diquark baryons.
- Some excited Λ_c states with a higher l have a similar or even larger production rate than the ground state, in particular $\Lambda_c(1/2^-)$ and $\Lambda_c(3/2^-)$, and $\Lambda_c(3/2^+)$ and $\Lambda_c(5/2^+)$. This is due to a large overlap of the wave functions when the momentum transfer is large, typically around 1 GeV for charm production. The momentum transfer value together with the size of the baryons determines an optimal angular momentum transfer Δl. For charm production this occurs at around $\Delta l \sim 1$, and for strangeness production at $\Delta l \ll 1$. Mathematically, this is explained by the combination of the power term $(q_{\rm eff}/A)^l$ and the form factor $\exp(-(q_{\rm eff}/2A)^2)$ as in Eqs. (A13) and (A16). In hypernucleus production, the same mechanism has been well appreciated, demonstrating the success in the studies of reaction and structure [23].
- The above pairs of Λ form a spin-orbit (LS) doublet in the quark model, or in the heavy quark limit the heavy quark doublet [24]. Their relative production rates are then determined in a model-independent manner up to a kinematic factor.
- We can similarly compute the amplitude for P (pseudoscalar)–Reggeon exchanges, by replacing the transverse spin by the longitudinal spin, $\vec{e}_\perp \cdot \vec{\sigma} \to \vec{e}_{||} \cdot \vec{\sigma}$. Although we do not consider this process in this paper, a unique feature is that V and P Reggeon exchanges do not interfere in the forward amplitude due to the spin selection rule.
- So far, we have looked at V ($= D^*$ or K^*) meson production due to the planned experimental requirements. Theoretically, we can also study the reactions followed by D or K meson production. In this case, pseudoscalar and scalar exchanges are possible, for which we can write down similar formulas.

4. Discussions and remarks

We have studied charm production induced by the high-momentum pion beam. This is a very challenging problem since no experiment has been performed for almost thirty years since the one at Brookhaven [11]. However, charmed baryon spectroscopy will bring us fruitful information for yet-unexplored regions in hadron physics. This has been the primary motivation of the present study.

We first estimated that in the Regge model charm production is suppressed by a factor of 10^{-4} as compared to strangeness production, implying an expected cross section of the order of 1 [nb]. Another important finding in the present study is that the production rates of excited charmed baryons are not necessarily suppressed as compared to those of the ground state. This is a consequence of good overlaps of the initial- and final-state baryons at the momentum transfer around 1 GeV, providing us with more opportunity for the study of excited states.

In the present study, we have used a simple quark and diquark model for baryons. In view of the successes of the constituent picture for low-lying states, we expect that some of the features should also persist in the charm production reactions. In particular, the identification of λ and ρ modes should be very important to reveal the mechanism of hadron excitations. Further investigations of the production and decay in the heavy quark region may provide good information on it.

Acknowledgements

We thank A. I. Titov, M. Oka, K. Sadato, and T. Yoshida for discussions. This work is supported in part by the Grant-in-Aid for Science Research (C) 26400273. S.H.K. is supported by a Scholarship of the Ministry of Education, Culture, Science and Technology of Japan. The work of H.-Ch.K. was supported by the Basic Science Research Program through the National Research Foundation of Korea funded by the Ministry of Education, Science and Technology (Grant Number: 2013S1A2A2035612).

Funding

Open Access funding: SCOAP[3].

Appendix A. Matrix elements

Let us calculate the matrix elements $\langle f | \vec{e}_\perp \cdot \vec{\sigma}\, e^{i\vec{q}_{\rm eff}\cdot\vec{x}} | i\rangle$ for baryons B with various spin and parity J^P. For forward scattering, due to helicity conservation, it is sufficient to consider only one helicity flip transition for a given J (remember that only transverse polarization transfer is possible),

$$i \to f = J_z(N) \to (J_z(B), h) = 1/2 \to (-1/2, 1) \tag{A1}$$

for $J = 1/2$ and 3/2, and

$$J_z(N) \to (J_z(B), h) = -1/2 \to (-3/2, 1) \tag{A2}$$

for $J = 3/2$. Here h denotes the helicity of the vector meson V. Other amplitudes are related to these elements by time reversal.

The total cross section is then proportional to the sum of squared amplitudes over possible spin states. For $J = 1/2$

$$\begin{aligned}\sigma &\sim |\langle -1/2, +1|t| + 1/2\rangle|^2 + |\langle +1/2, -1|t| - 1/2\rangle|^2 \\ &= 2|\langle -1/2, +1|t| + 1/2\rangle|^2\end{aligned} \tag{A3}$$

and for $J = 3/2$ and 5/2

$$\sigma \sim 2\big(|\langle -1/2, +1|t| + 1/2\rangle|^2 + |\langle +3/2, -1|t| + 1/2\rangle|^2\big). \tag{A4}$$

A.1. $N(1/2^+) \to$ *ground-state baryons*

First we consider the transition to $\Lambda(1/2^+)$ (of both charm and strangeness)

$$\big\langle \psi_{000}\chi^\rho_{-1/2} V(+1)\big|\vec{e}_\perp \cdot \vec{\sigma}\, e^{i\vec{q}_{\rm eff}\cdot\vec{x}}\,\big|\psi_{000}\chi^\rho_{+1/2}\big\rangle, \tag{A5}$$

where the baryon orbital wave functions ψ_{nlm} are given in Appendix C. Note that since the diquark behaves as a spectator in the reaction (Fig. 1), the good diquark component of χ^ρ for the nucleon is taken. The spectroscopic (overlap) factor of the good diquark component in the nucleon is tabulated below, where the isospin factor is also included. Choosing the V polarization as $\vec{e}_\perp$, we have

$$\big\langle \psi_{000}\chi^\rho_{-1/2}\big|\sqrt{2}\sigma_-\, e^{i\vec{q}_{\rm eff}\cdot\vec{x}}\,\big|\psi_{000}\chi^\rho_{+1/2}\big\rangle = \big\langle \chi^\rho_{-1/2}|\sigma_-|\chi^\rho_{+1/2}\big\rangle \big\langle \psi_{000}\big|\sqrt{2}\, e^{i\vec{q}_{\rm eff}\cdot\vec{x}}\,\big|\psi_{000}\big\rangle, \tag{A6}$$

where the spin and orbital parts are separated and σ_- is the spin-lowering matrix given as

$$\sigma_- = \begin{pmatrix} 0 & 0 \\ 1 & 0 \end{pmatrix}. \tag{A7}$$

The spin matrix elements are easily computed as

$$\begin{aligned}
\left\langle \chi^{\rho}_{-1/2} | \sigma_- | \chi^{\rho}_{+1/2} \right\rangle &= 1, \\
\left\langle \chi^{\lambda}_{-1/2} | \sigma_- | \chi^{\lambda} + 1/2 \right\rangle &= -\frac{1}{3}, \\
\left\langle \chi^{S}_{-1/2} | \sigma_- | \chi^{\lambda} + 1/2 \right\rangle &= \frac{\sqrt{2}}{3}, \\
\left\langle \chi^{S}_{-3/2} | \sigma_- | \chi^{\lambda} - 1/2 \right\rangle &= -\sqrt{\frac{2}{3}},
\end{aligned} \tag{A8}$$

where we have shown all relevant matrix elements in the following calculations. Therefore, the remaining is the elementary integral over the radial distance r with Gaussian functions. We find

$$\Lambda(1/2^+): \quad \left\langle \psi_{000} \chi^{\rho}_{-1/2} \right| \sqrt{2} \sigma_- \, e^{i \vec{q}_{\rm eff} \cdot \vec{x}} \left| \psi_{000} \chi^{\rho}_{+1/2} \right\rangle = I_0, \tag{A9}$$

where the radial integral I_0 is given by

$$\begin{aligned}
I_0 &= \left\langle \psi_{000} \right| \sqrt{2} \, e^{i \vec{q}_{\rm eff} \cdot \vec{x}} \left| \psi_{000} \right\rangle = \sqrt{2} \left(\frac{\alpha' \alpha}{A^2} \right)^{3/2} e^{-q^2_{\rm eff}/(4A^2)}, \\
A^2 &= \frac{\alpha^2 + \alpha'^2}{2}.
\end{aligned} \tag{A10}$$

The oscillator parameters are α and α' are for the initial- and final-state baryons, respectively.

Similarly, we calculate the transitions to the ground-state Σ, picking up the χ^{λ} part for the nucleon wave function. The only difference is the spin matrix element, which is computed by making Clebsch–Gordan decompositions. The results are

$$\begin{aligned}
\Sigma(1/2^+): \quad & \left\langle \psi_{000} \chi^{\lambda}_{-1/2} \right| \sqrt{2} \sigma_- \, e^{i \vec{q}_{\rm eff} \cdot \vec{x}} \left| \psi_{000} \chi^{\lambda}_{+1/2} \right\rangle = -\tfrac{1}{3} I_0, \\
\Sigma(3/2^+): \quad & \left\langle \psi_{000} \chi^{S}_{-1/2} \right| \sqrt{2} \sigma_- \, e^{i \vec{q}_{\rm eff} \cdot \vec{x}} \left| \psi_{000} \chi^{\lambda}_{+1/2} \right\rangle = \tfrac{\sqrt{2}}{3} I_0, \\
& \left\langle \psi_{000} \chi^{S}_{-3/2} \right| \sqrt{2} \sigma_- \, e^{i \vec{q}_{\rm eff} \cdot \vec{x}} \left| \psi_{000} \chi^{\lambda}_{-1/2} \right\rangle = -\sqrt{\tfrac{2}{3}} I_0,
\end{aligned} \tag{A11}$$

where two independent matrix elements for $\Sigma(3/2^+)$ are shown.

A.2. $N(1/2^+) \to$ p-wave baryons

Let us first consider the transition to $\Lambda(1/2^-)$. The relevant matrix element is given as

$$\left\langle \left[\psi_{01}, \chi^{\rho} \right]^{1/2}_{-1/2} \right| \sqrt{2} \sigma_- \, e^{i \vec{q}_{\rm eff} \cdot \vec{x}} \left| \psi_{000} \chi^{\rho}_{+1/2} \right\rangle = \sqrt{\tfrac{1}{3}} \left\langle \chi^{\rho}_{-1/2} | \sigma_- | \chi^{\rho}_{+1/2} \right\rangle \left\langle \psi_{010} \right| \sqrt{2} \, e^{i \vec{q}_{\rm eff} \cdot \vec{x}} \left| \psi_{000} \right\rangle, \tag{A12}$$

where the factor $\sqrt{1/3}$ is the Clebsch–Gordan coefficients in the state $[\psi_{01}, \chi^{\rho}]^{1/2}_{-1/2}$. The radial part is computed as

$$\left\langle \psi_{010} \right| \sqrt{2} \, e^{i \vec{q}_{\rm eff} \cdot \vec{x}} \left| \psi_{000} \right\rangle = \frac{(\alpha' \alpha)^{3/2} \alpha' q_{\rm eff}}{A^5} e^{-q^2_{\rm eff}/(4A^2)} \equiv I_1 \tag{A13}$$

and so

$$\Lambda(1/2^-): \quad \left\langle [\psi_{01}, \chi^{\rho}]^{1/2}_{-1/2} \right| \sqrt{2} \sigma_- \, e^{i \vec{q}_{\rm eff} \cdot \vec{x}} \left| \psi_{000} \chi^{\rho}_{+1/2} \right\rangle = \sqrt{\tfrac{1}{3}} \, I_1. \tag{A14}$$

Other matrix elements can be computed similarly:

$$
\begin{aligned}
\Lambda(3/2^-): \quad & \left\langle \left[\psi_{01},\chi^\rho\right]^{3/2}_{-1/2}\middle|\sqrt{2}\sigma_- \, e^{i\vec{q}_{\rm eff}\cdot\vec{x}}\,\middle|\psi_{000}\chi^\rho_{+1/2}\right\rangle = \sqrt{\tfrac{2}{3}}I_1, \\
& \left\langle \left[\psi_{01},\chi^\rho\right]^{3/2}_{-3/2}\middle|\sqrt{2}\sigma_- \, e^{i\vec{q}_{\rm eff}\cdot\vec{x}}\,\middle|\psi_{000}\chi^\rho_{-1/2}\right\rangle = 0, \\
\Sigma(1/2^-): \quad & \left\langle \left[\psi_{01},\chi^\lambda\right]^{3/2}_{-1/2}\middle|\sqrt{2}\sigma_- \, e^{i\vec{q}_{\rm eff}\cdot\vec{x}}\,\middle|\psi_{000}\chi^\lambda_{+1/2}\right\rangle = \tfrac{1}{3\sqrt{3}}I_1, \\
\Sigma(3/2^-): \quad & \left\langle \left[\psi_{01},\chi^\lambda\right]^{3/2}_{-1/2}\middle|\sqrt{2}\sigma_- \, e^{i\vec{q}_{\rm eff}\cdot\vec{x}}\,\middle|\psi_{000}\chi^\lambda_{+1/2}\right\rangle = -\tfrac{1}{3}\sqrt{\tfrac{2}{3}}I_1, \\
& \left\langle \left[\psi_{01},\chi^\lambda\right]^{3/2}_{-3/2}\middle|\sqrt{2}\sigma_- \, e^{i\vec{q}_{\rm eff}\cdot\vec{x}}\,\middle|\psi_{000}\chi^\lambda_{-1/2}\right\rangle = 0, \\
\Sigma'(1/2^-): \quad & \left\langle \left[\psi_{01},\chi^S\right]^{1/2}_{-1/2}\middle|\sqrt{2}\sigma_- \, e^{i\vec{q}_{\rm eff}\cdot\vec{x}}\,\middle|\psi_{000}\chi^\lambda_{+1/2}\right\rangle = -\tfrac{1}{3}\sqrt{\tfrac{2}{3}}I_1, \\
\Sigma'(3/2^-): \quad & \left\langle \left[\psi_{01},\chi^S\right]^{3/2}_{-1/2}\middle|\sqrt{2}\sigma_- \, e^{i\vec{q}_{\rm eff}\cdot\vec{x}}\,\middle|\psi_{000}\chi^\lambda_{+1/2}\right\rangle = \tfrac{1}{3}\sqrt{\tfrac{2}{15}}I_1, \\
& \left\langle \left[\psi_{01},\chi^S\right]^{3/2}_{-3/2}\middle|\sqrt{2}\sigma_- \, e^{i\vec{q}_{\rm eff}\cdot\vec{x}}\,\middle|\psi_{000}\chi^\lambda_{-1/2}\right\rangle = \sqrt{\tfrac{2}{5}}I_1, \\
\Sigma'(5/2^-): \quad & \left\langle \left[\psi_{01},\chi^S\right]^{5/2}_{-1/2}\middle|\sqrt{2}\sigma_- \, e^{i\vec{q}_{\rm eff}\cdot\vec{x}}\,\middle|\psi_{000}\chi^\lambda_{+1/2}\right\rangle = -\sqrt{\tfrac{2}{15}}I_1, \\
& \left\langle \left[\psi_{01},\chi^S\right]^{5/2}_{-3/2}\middle|\sqrt{2}\sigma_- \, e^{i\vec{q}_{\rm eff}\cdot\vec{x}}\,\middle|\psi_{000}\chi^\lambda_{-1/2}\right\rangle = -\sqrt{\tfrac{4}{15}}I_1.
\end{aligned}
\tag{A15}
$$

A.3. $N(1/2^+) \to$ *d-wave baryons*

The computations go in a completely similar manner to before, except for the radial matrix element

$$
\left\langle \psi_{020}\middle|\sqrt{2}\, e^{i\vec{q}_{\rm eff}\cdot\vec{x}}\,\middle|\psi_{000}\right\rangle = \tfrac{1}{2}\sqrt{\tfrac{2}{3}}\frac{(\alpha\alpha')^{3/2}}{A^3}\left(\frac{\alpha' q}{A^2}\right)^2 e^{-q^2_{\rm eff}/(4A^2)} \equiv I_2. \tag{A16}
$$

The results are

$$
\begin{aligned}
\Lambda(3/2^+): \quad & \left\langle \left[\psi_{02},\chi^\rho\right]^{3/2}_{-1/2}\middle|\sqrt{2}\sigma_- \, e^{i\vec{q}_{\rm eff}\cdot\vec{x}}\,\middle|\psi_{000}\chi^\rho_{+1/2}\right\rangle = -\sqrt{\tfrac{2}{5}}I_2, \\
& \left\langle \left[\psi_{02},\chi^\rho\right]^{3/2}_{-3/2}\middle|\sqrt{2}\sigma_- \, e^{i\vec{q}_{\rm eff}\cdot\vec{x}}\,\middle|\psi_{000}\chi^\rho_{-1/2}\right\rangle = 0, \\
\Lambda(5/2^+): \quad & \left\langle \left[\psi_{02},\chi^\rho\right]^{5/2}_{-1/2}\middle|\sqrt{2}\sigma_- \, e^{i\vec{q}_{\rm eff}\cdot\vec{x}}\,\middle|\psi_{000}\chi^\rho_{+1/2}\right\rangle = \sqrt{\tfrac{3}{5}}I_2, \\
& \left\langle \left[\psi_{02},\chi^\rho\right]^{5/2}_{-3/2}\middle|\sqrt{2}\sigma_- \, e^{i\vec{q}_{\rm eff}\cdot\vec{x}}\,\middle|\psi_{000}\chi^\rho_{-1/2}\right\rangle = 0, \\
\Sigma(3/2^+): \quad & \left\langle \left[\psi_{02},\chi^\lambda\right]^{3/2}_{-1/2}\middle|\sqrt{2}\sigma_- \, e^{i\vec{q}_{\rm eff}\cdot\vec{x}}\,\middle|\psi_{000}\chi^\lambda_{+1/2}\right\rangle = \sqrt{\tfrac{3}{5}}I_2, \\
& \left\langle \left[\psi_{02},\chi^\lambda\right]^{3/2}_{-3/2}\middle|\sqrt{2}\sigma_- \, e^{i\vec{q}_{\rm eff}\cdot\vec{x}}\,\middle|\psi_{000}\chi^\lambda_{-1/2}\right\rangle = 0, \\
\Sigma(5/2^+): \quad & \left\langle \left[\psi_{02},\chi^\lambda\right]^{5/2}_{-1/2}\middle|\sqrt{2}\sigma_- \, e^{i\vec{q}_{\rm eff}\cdot\vec{x}}\,\middle|\psi_{000}\chi^\lambda_{+1/2}\right\rangle = \sqrt{\tfrac{3}{5}}I_2, \\
& \left\langle \left[\psi_{02},\chi^\lambda\right]^{5/2}_{-3/2}\middle|\sqrt{2}\sigma_- \, e^{i\vec{q}_{\rm eff}\cdot\vec{x}}\,\middle|\psi_{000}\chi^\lambda_{-1/2}\right\rangle = 0,
\end{aligned}
$$

$$
\begin{aligned}
\Sigma'(1/2^+): \quad & \left\langle \left[\psi_{02}, \chi^S\right]^{1/2}_{-1/2} \middle| \sqrt{2}\sigma_- e^{i\vec{q}_{\rm eff}\cdot\vec{x}} \middle| \psi_{000}\chi^\lambda_{+1/2}\right\rangle = \sqrt{\tfrac{3}{5}} I_2, \\
\Sigma'(3/2^+): \quad & \left\langle \left[\psi_{02}, \chi^S\right]^{3/2}_{-1/2} \middle| \sqrt{2}\sigma_- e^{i\vec{q}_{\rm eff}\cdot\vec{x}} \middle| \psi_{000}\chi^\lambda_{+1/2}\right\rangle = \sqrt{\tfrac{3}{5}} I_2, \\
& \left\langle \left[\psi_{02}, \chi^S\right]^{3/2}_{-3/2} \middle| \sqrt{2}\sigma_- e^{i\vec{q}_{\rm eff}\cdot\vec{x}} \middle| \psi_{000}\chi^\lambda_{-1/2}\right\rangle = 0, \\
\Sigma'(5/2^+): \quad & \left\langle \left[\psi_{02}, \chi^S\right]^{5/2}_{-1/2} \middle| \sqrt{2}\sigma_- e^{i\vec{q}_{\rm eff}\cdot\vec{x}} \middle| \psi_{000}\chi^\lambda_{+1/2}\right\rangle = \sqrt{\tfrac{3}{5}} I_2, \\
& \left\langle \left[\psi_{02}, \chi^S\right]^{5/2}_{-3/2} \middle| \sqrt{2}\sigma_- e^{i\vec{q}_{\rm eff}\cdot\vec{x}} \middle| \psi_{000}\chi^\lambda_{-1/2}\right\rangle = 0, \\
\Sigma'(7/2^+): \quad & \left\langle \left[\psi_{02}, \chi^S\right]^{7/2}_{-1/2} \middle| \sqrt{2}\sigma_- e^{i\vec{q}_{\rm eff}\cdot\vec{x}} \middle| \psi_{000}\chi^\lambda_{+1/2}\right\rangle = \sqrt{\tfrac{3}{5}} I_2, \\
& \left\langle \left[\psi_{02}, \chi^S\right]^{7/2}_{-3/2} \middle| \sqrt{2}\sigma_- e^{i\vec{q}_{\rm eff}\cdot\vec{x}} \middle| \psi_{000}\chi^\lambda_{-1/2}\right\rangle = 0. \qquad \text{(A17)}
\end{aligned}
$$

Appendix B. Baryon wave functions

We summarize the baryon wave functions used in the present calculations [25]. They are constructed by a quark and a diquark, and are expressed as products of isospin, spin, and orbital wave functions. Here we show explicitly the spin and orbital parts. For orbital wave functions, we employ harmonic oscillator functions as given in Appendix C.

For spin wave functions, using the notation for angular momentum coupling $[L_1, L_2]^{L_{\rm tot}}$, we employ the three functions

$$
\begin{aligned}
\chi^\rho_m &= [d^0, \chi]^{1/2}_m, \\
\chi^\lambda_m &= [d^1, \chi]^{1/2}_m, \\
\chi^S_m &= [d^1, \chi]^{3/2}_m, \qquad \text{(B1)}
\end{aligned}
$$

where d^S denotes the diquark spin function, and χ the two-component spinor for a single quark. For the ground baryons we have three states:

$$
\begin{aligned}
\Lambda(1/2^+, m) &= \psi_{000}(\vec{x})\chi^\rho_m, \\
\Sigma(1/2^+, m) &= \psi_{000}(\vec{x})\chi^\lambda_m, \\
\Sigma(3/2^+, m) &= \psi_{000}(\vec{x})\chi^S_m. \qquad \text{(B2)}
\end{aligned}
$$

For the first excited states of negative parity there are seven states ($\psi_{nlm} \to \psi_{nl} = \psi_{01}$):

$$
\begin{aligned}
\Lambda(1/2^-, m) &= [\psi_{01}(\vec{x}), \chi^\rho]^{1/2}_m, \\
\Lambda(3/2^-, m) &= [\psi_{01}(\vec{x}), \chi^\rho]^{3/2}_m, \\
\Sigma(1/2^-, m) &= [\psi_{01}(\vec{x}), \chi^\lambda]^{1/2}_m, \\
\Sigma(3/2^-, m) &= [\psi_{01}(\vec{x}), \chi^\lambda]^{3/2}_m, \\
\Sigma'(1/2^-, m) &= [\psi_{01}(\vec{x}), \chi^S]^{1/2}_m, \\
\Sigma'(3/2^-, m) &= [\psi_{01}(\vec{x}), \chi^S]^{3/2}_m, \\
\Sigma'(5/2^-, m) &= [\psi_{01}(\vec{x}), \chi^S]^{5/2}_m. \qquad \text{(B3)}
\end{aligned}
$$

Similarly, we obtain the wave functions for the $l = 2$ excited baryons.

Finally, the nucleon wave function is given as

$$N = \psi_{000} \frac{1}{\sqrt{2}} \left(\chi^{\rho} \phi^{\rho} + \chi^{\lambda} \phi^{\lambda} \right), \tag{B4}$$

where ϕ^{ρ} and ϕ^{λ} are the isospin 1/2 wave functions of the nucleon with three quarks.

Appendix C. Harmonic oscillator wave functions

We summarize some of the harmonic oscillator wave functions for low-lying states. Including the angular and radial parts, they are given as

$$\psi_{nlm}(\vec{x}) = Y_{lm}(\hat{x}) R_{nl}(r), \tag{C1}$$

where $R_{nl}(r)$ are

$$\begin{aligned}
R_{00}(r) &= \frac{\alpha^{3/2}}{\pi^{1/4}} 2 e^{-(\alpha^2/2) r^2}, \\
R_{01}(r) &= \frac{\alpha^{3/2}}{\pi^{1/4}} \left(\frac{8}{3} \right)^{1/2} \alpha r e^{-(\alpha^2/2) r^2}, \\
R_{10}(r) &= \frac{\alpha^{3/2}}{\pi^{1/4}} (2 \cdot 3)^{1/2} \left(1 - \frac{2}{3} (\alpha r)^2 \right) e^{-(\alpha^2/2) r^2}, \\
R_{02}(r) &= \frac{\alpha^{3/2}}{\pi^{1/4}} \left(\frac{16}{5 \cdot 3} \right)^{1/2} (\alpha r)^2 e^{-(\alpha^2/2) r^2}.
\end{aligned} \tag{C2}$$

The oscillator parameter α is related to the frequency ω by

$$\alpha = \sqrt{m\omega} = (km)^{1/4}, \tag{C3}$$

where k is the spring constant.

References

[1] N. Brambilla et al., Eur. Phys. J. C **71**, 1534 (2011).
[2] S. K. Choi et al. [Belle Collaboration], Phys. Rev. Lett. **91**, 262001 (2003).
[3] B. Aubert et al. [BaBar Collaboration], Phys. Rev. D **71**, 071103 (2005).
[4] S. K. Choi et al. [BELLE Collaboration], Phys. Rev. Lett. **100**, 142001 (2008) [arXiv:0708.1790 [hep-ex]].
[5] A. Bondar et al. [Belle Collaboration], Phys. Rev. Lett. **108**, 122001 (2012) [arXiv:1110.2251 [hep-ex]].
[6] M. Ablikim et al. [BESIII Collaboration], Phys. Rev. Lett. **110**, 252001 (2013).
[7] Z. Q. Liu et al. [Belle Collaboration], Phys. Rev. Lett. **110**, 252002 (2013).
[8] R. Aaij et al. [LHCb Collaboration], Phys. Rev. Lett. **110**, 222001 (2013).
[9] R. Aaij et al. [LHCb Collaboration], arXiv:1404.1903 [hep-ex].
[10] *Charmed baryon spectroscopy via the* (π^-, D^{*-}) *reaction* (2012). (Available at: http://www.j-parc.jp/researcher/Hadron/en/Proposal_e.html#1301). J-PARC P50 proposal.
[11] J. H. Christenson, E. Hummel, G. A. Kreiter, J. Sculli, and P. Yamin, Phys. Rev. Lett. **55**, 154 (1985).
[12] L. A. Copley, N. Isgur, and G. Karl, Phys. Rev. D **20**, 768 (1979); **23**, 817 (1981) [erratum].
[13] W. Roberts and M. Pervin, Int. J. Mod. Phys. A **23**, 2817 (2008) [arXiv:0711.2492 [nucl-th]].
[14] O. I. Dahl, L. M. Hardy, R. I. Hess, J. Kirz, and D. H. Miller, Phys. Rev. **163**, 1377 (1967).
[15] D. J. Crennell, H. A. Gordon, K.-W. Lai, and J. M. Scarr, Phys. Rev. D **6**, 1220 (1972).
[16] A. Donnachie, H. G. Dosch, P. V. Landshoff, and O. Nachtmann, *Pomeron Physics and QCD* (Cambridge University Press, Cambridge, UK, 2002).
[17] A. B. Kaidalov, Z. Phys. C **12**, 63 (1982).
[18] A. B. Kaidalov and P. E. Volkovitsky, Z. Phys. C **63**, 517 (1994).
[19] M. M. Brisudova, L. Burakovsky, and J. T. Goldman, Phys. Rev. D **61**, 054013 (2000).
[20] V. Y. Grishina, L. A. Kondratyuk, W. Cassing, M. Mirazita, and P. Rossi, Eur. Phys. J. A **25**, 141 (2005).

[21] A. I. Titov and B. Kampfer, Phys. Rev. C **78**, 025201 (2008).
[22] J. Beringer et al. [Particle Data Group Collaboration], Phys. Rev. D **86**, 010001 (2012) [http://pdg.lbl.gov].
[23] K. Itonaga, T. Motoba, and H. Bando, Prog. Theor. Phys. **84**, 291 (1990).
[24] Y. Yamaguchi, S. Ohkoda, A. Hosaka, T. Hyodo, and S. Yasui, arXiv:1402.5222 [hep-ph].
[25] A. Hosaka and H. Toki, *Quarks, Baryons and Chiral Symmetry* (World Scientific, Singapore, 2001).